

Discovery of CDZ173 (leniolisib), Representing a Structurally Novel Class of PI3K Delta-Selective Inhibitors

Klemens Hoegenauer, Nicolas Soldermann, Frederic Zecri, Ross S. Strang, Nadege Graveleau, Romain M Wolf, Nigel G. Cooke, Alexander B. Smith, Gregory J. Hollingworth, Joachim Blanz, Sascha Gutmann, Gabriele Rummel, Amanda Littlewood-Evans, and Christoph Burkhardt

ACS Med. Chem. Lett., **Just Accepted Manuscript** • DOI: 10.1021/acsmedchemlett.7b00293 • Publication Date (Web): 25 Aug 2017

Downloaded from <http://pubs.acs.org> on August 29, 2017

Just Accepted

"Just Accepted" manuscripts have been peer-reviewed and accepted for publication. They are posted online prior to technical editing, formatting for publication and author proofing. The American Chemical Society provides "Just Accepted" as a free service to the research community to expedite the dissemination of scientific material as soon as possible after acceptance. "Just Accepted" manuscripts appear in full in PDF format accompanied by an HTML abstract. "Just Accepted" manuscripts have been fully peer reviewed, but should not be considered the official version of record. They are accessible to all readers and citable by the Digital Object Identifier (DOI®). "Just Accepted" is an optional service offered to authors. Therefore, the "Just Accepted" Web site may not include all articles that will be published in the journal. After a manuscript is technically edited and formatted, it will be removed from the "Just Accepted" Web site and published as an ASAP article. Note that technical editing may introduce minor changes to the manuscript text and/or graphics which could affect content, and all legal disclaimers and ethical guidelines that apply to the journal pertain. ACS cannot be held responsible for errors or consequences arising from the use of information contained in these "Just Accepted" manuscripts.



Discovery of CDZ173 (leniolisib), Representing a Structurally Novel Class of PI3K Delta-Selective Inhibitors

Klemens Hoegenauer^a, Nicolas Soldermann^a, Frédéric Zécari^a, Ross S. Strang^a, Nadege Graveleau^a, Romain M. Wolf^a, Nigel G. Cooke^a, Alexander B. Smith^a, Gregory J. Hollingworth^a, Joachim Blanz^b, Sascha Gutmann^c, Gabriele Rummel^c, Amanda Littlewood-Evans^d, Christoph Burkhardt^d

^aGlobal Discovery Chemistry, ^bPK Sciences, ^cChemical Biology and Therapeutics, ^dAutoimmunity, Transplantation and Inflammation, Novartis Institutes for BioMedical Research, Novartis Campus, CH-4002 Basel, Switzerland

ABSTRACT: The predominant expression of Phosphoinositide 3-kinase δ (PI3K δ) in leukocytes and its critical role in B and T cell functions led to the hypothesis that selective inhibitors of this isoform would have potential as therapeutics for the treatment of allergic and inflammatory disease. Targeting specifically PI3K δ should avoid potential side effects associated with the ubiquitously expressed PI3K α and β isoforms. We disclose how morphing the heterocyclic core of previously discovered 4,6-diaryl quinazolines to a significantly less lipophilic 5,6,7,8-tetrahydropyrido[4,3-d]pyrimidine, followed by replacement of one of the phenyl groups with a pyrrolidine-3-amine, led to a compound series with optimal on-target profile and good ADME properties. A final lipophilicity adjustment led to the discovery of CDZ173 (leniolisib), a potent PI3K δ selective inhibitor with suitable properties and efficacy for clinical development as an anti-inflammatory therapeutic. *In vitro*, CDZ173 inhibits a large spectrum of immune cell functions, as demonstrated in B and T cells, neutrophils, monocytes, basophils, plasmacytoid dendritic cells and mast cells. *In vivo*, CDZ173 inhibits B cell activation in rats and monkeys in a concentration- and time-dependent manner. After prophylactic or therapeutic dosing, CDZ173 potently inhibited antigen-specific antibody production and reduced disease symptoms in a rat collagen-induced arthritis model. Structurally, CDZ173 differs significantly from the first generation of PI3K δ and PI3K $\gamma\delta$ -selective clinical compounds. Therefore, CDZ173 could differentiate by a more favorable safety profile. CDZ173 is currently in clinical studies in patients suffering from primary Sjögren's syndrome and in APDS/PASLI, a disease caused by gain-of-function mutations of PI3K δ .

KEYWORDS Phosphoinositide-3-kinase delta inhibitor, PI3K δ inhibitor, lead optimization, structure-activity relationship, PK/PD studies, B cell inhibition

Phosphoinositide-3-kinase δ (PI3K δ) is a lipid kinase composed of an enzymatic p110 δ subunit and a regulatory p85 subunit expressed predominantly in hematopoietic cells. PI3K δ catalyzes the intracellular conversion of phosphatidylinositol 4,5-bisphosphate (PIP2) to phosphatidylinositol 3,4,5-trisphosphate (PIP3) downstream of a number of receptor tyrosine kinases (eg. BCR, TCR, Fc ϵ R1)^{1,2} as well as some G protein-coupled receptors (GPCR; eg. CXCR5).³

Inhibition of PI3K δ has been shown to be beneficial for the treatment of hematological malignancies where the PI3K/AKT path-

way is hyperactive.^{4,5} The importance of PI3K δ for the function of cells involved in inflammatory respiratory diseases (T cells, mast cells, neutrophils)^{6–8} has guided the development of inhaled and oral PI3K δ inhibitors for the treatment of asthma or chronic obstructive pulmonary disease.^{9–11} Moreover, PI3K δ is overactive in patients with autoimmune diseases such as rheumatoid arthritis¹² and systemic lupus erythematosus,^{13,14} where PI3K δ inhibitors have been effective in respective murine models.^{15,16} In patients with Activated PI3K δ Syndrome (APDS), mutations in the PIK3CD gene encoding p110 δ lead to an immunodeficiency characterized by recurrent infections and prominent lymphoproliferation.^{17,18} In summary, there is strong evidence that PI3K δ inhibition is a promising therapeutic principle for the treatment of APDS as well as inflammatory and autoimmune diseases,^{19–21} prompting numerous companies to engage in programs geared towards the identification of potent and selective PI3K δ inhibitors.^{11,22–29}

We have recently disclosed the optimization of novel 4,6-diaryl quinazolines as PI3K δ -selective inhibitors.³⁰ These efforts led to discovery of quinazoline **1a** as a potent and isoform selective inhibitor of PI3K δ (Table 1). We could demonstrate that compound **1a** is effective in down-regulating PI3K δ -mediated signaling *in vitro* and *in vivo*, ultimately resulting in dose-dependent efficacy in a mechanistic rodent model after oral dosing. However, when amorphous material of compound **1a** was exposed to an aqueous environment, a crystalline trihydrate polymorph formed over time. This trihydrate had low aqueous solubility, and we hypothesized that solubility-limited absorption was the reason for the underproportional exposure increase which we observed with compound **1a** in higher dose rat PK studies.³⁰ When we directly compared trihydrate vs amorphous material in rat PK studies, we indeed observed a significant drop in exposure (ca. 5-fold, data not shown). A polymorph with poor aqueous solubility that is formed under an aqueous environment poses a serious development hurdle as inconsistent or erratic exposure levels become more likely. This not only impacts preclinical efficacy or toxicological studies, but also poses a risk in later clinical development (safety risk if exposure is too high, lacking efficacy risk if too low). It became the project goal to identify a replacement for compound **1a** with an improved solubility of crystalline material.

We recently disclosed that the 4-aryl spacer could be substituted by a pyrrolidineoxy substituent which led to an improved membrane permeability profile and increased ligand efficiency.³¹ When the core quinazoline was changed to other heterocycles that still contained the hinge binding nitrogen, namely quinolines, 1,5-naphthyridines and cinnolines, we observed that a substantial modulation of the lipophilicity was the consequence. Not every

derivative, including the compounds that are presented in this manuscript, showed a tight correlation of log D with other parameters that are known to be modulated by lipophilicity, such as solubility, membrane permeability and microsomal stability. Nevertheless we noticed some consistent impact by lipophilicity changes which we outline in the following section.

As part of our core scaffold modifications we extended our investigations to partially saturated bicyclic systems, and in this context we discovered 5,6,7,8-tetrahydropyrido[4,3-d]pyrimidine (THPP) as a suitable core that decreased lipophilicity significantly. This is illustrated by comparing quinazoline **1b** (HT-logP = 2.7) to the similarly substituted THPP analogue **2a** (HT-logP = 0.7); the lipophilicity drop of two orders of magnitude resulted in a marked decrease of membrane permeability (PAMPA log Pe = $-4.9 \cdot 10^{-6}$ → $6.7 \cdot 10^{-6}$ cm·sec⁻¹ at pH = 6.8), and a loss in cellular activity (PI3Kδ IC₅₀ = 2.63 μM). Replacing one of the amide bonds by an ether bridge (**2a**→**2b**) increased lipophilicity (HT-logP = 2.2), reduced topological polar surface area (tPSA = 91 → 80 Å²), improved membrane permeability, and the biochemical activity translates better into cellular assays. When we introduced the pyrrolidineoxy-substituents on the THPP core we found that the overall biochemical and cellular PI3Kδ activities for our first analogues such as **3a** were moderate. At the same time, the lipophilicity space appeared highly promising, and ADME properties such as membrane permeability, solubility and stability in liver microsomes were favourable. By SAR expansion we learned that introducing a CF₃ group in the 3-position of the methoxypyridine (**3a**→**3b**) increased PI3Kδ potency by a factor of five. This modification was accompanied by a lipophilicity increase by almost one order of magnitude, and solubility and microsomal stability were negatively impacted. For oxygen-linked derivatives (**3a-d**), the optimal balance was found combining a methyl group in the 3-position of the pyridine with a tetrahydropyran group as R² substituent (compound **3c**). Similar to the pair **3a/3b**, an introduction of a CF₃ group (**3c**→**3d**) led to an increased *in vitro* clearance and reduced solubility.

When we switched the ether linker to an amine (**3e-h**), two ADME parameters were markedly affected: reduced *in vitro* clearance and reduced PAMPA permeability (compare compounds **3b** vs **3h**, **3c** vs **3e** and **3d** vs **3f**). In general, amine-linked analogues were also chemically more stable towards acid catalyzed hydrolysis compared to their oxygen-linked counterparts. In contrast to the oxygen-linked derivatives, the optimal overall property space for amine-linked analogues was achieved by a more lipophilic R¹/R² substitution pattern, such as that shown for propionamide derivatives **3g** and **3h**. Compound **3h** was found to have the optimal profile, hydrophilic enough to ensure good solubility and metabolic stability, yet not too polar to allow for favorable membrane permeability. This compound was selected for further profiling and later became our clinical candidate now known as CDZ173 (leniolisib).

Compared to compound **1a**, CDZ173 is similar with respect to the overall on-target/selectivity profile, moderate rat liver microsomal turnover and solubility of amorphous material. In contrast to compound **1a**, CDZ173 shows good PAMPA permeability, enabling favourable absorption as we will discuss later. In addition, the solubility of crystalline CDZ173 (free base) was sufficient to support all pharmacological and early toxicological experiments. At a later stage, a crystalline phosphate salt with an >500-fold solubility improvement was identified in a salt screen (see Supplementary Table 1) and chosen as clinical service form in order to reduce the risk for exposure variability and/or food effects.

At the time when the optimization work was conducted, we did not have any x-ray co-crystal structures for PI3Kδ selective ligands. As a surrogate, we used a homology model based on PI3Kγ. As this model was not able to explain the reasons for the observed

selectivity, we optimized PI3K activity empirically using biochemical and cellular assay results.³¹ The first structures of selective ligands complexed with PI3Kδ became available only after CDZ173 had been identified. It was only at this point that a solid selectivity rationale on the molecular level could be developed (Figure 1). A comparison of the structures of quinazoline **1** bound to PI3Kα and PI3Kδ revealed differences in the binding modes of the inhibitor to the ATP sites of both isoforms.³⁰ Whereas the acetyl-piperazine group of the ligand stacks to the side chain of W760 in PI3Kδ, the corresponding interaction to W780 in PI3Kα is prevented by R770 in PI3Kα and the ligand is bound in an extended conformation to this isoform (Figure 1, left panel). This loss of Van der Waals interactions between the inhibitor and W780 in PI3Kα correlates with considerable loss in potency of the inhibitor for PI3Kα compared to PI3Kδ. We hypothesized that maintaining the stacking interaction with W760 (PI3Kδ) while preventing the ligand from adopting an extended conformation would offer a design principle for PI3Kδ inhibitors with exquisite selectivity over PI3Kα. To test this hypothesis, we obtained the co-crystal structure of CDZ173 bound to the ATP site of PI3Kδ (Figure 1, right panel). This structure reveals that the propionamide group of CDZ173 stacks with W760 in a similar way to the acetyl-piperazine group of compound **1a**. This binding mode of CDZ173 confirms our docking results,³¹ and strengthens our hypothesis that the (S)-enantiomer is preferred regarding PI3Kδ potency and isoform selectivity. Supplementary Figure 10 shows that the binding modes observed for compounds **1a** and CDZ173 clearly differ from previously discovered PI3Kδ inhibitors. “Propeller-shaped” inhibitors such as GS-643624 bind to a pocket that is induced by insertion of the quinazoline group of GS-643624 between W760 (PI3Kδ) and M752 (PI3Kδ) (“WM-pocket”).³² In the co-crystal structures of compounds **1** and CDZ173, M752 (PI3Kδ) occupies the area where the quinazoline of GS-643624 is bound. The WM-pocket is not induced for our inhibitor series.

As outlined in Table 1, the inhibitory effect on PI3Kα, β and δ isoforms on the cellular level was routinely assessed in Rat-1 cells transfected with human myr-p110 PI3K isoforms using the PI3K-dependent phosphorylation of AKT (pAKT) as a readout. The PI3Kδ activity of CDZ173 in this artificial assay system translated well into rodent B-cell activation assays (murine splenocytes and rat whole blood), indicating sufficient fraction unbound and minimal unspecific binding (Table 1). CDZ173 potently inhibits formation of proximal pathway markers (pAKT) and also anti-IgM+IL-4-induced expression of distal markers of B cell activation (CD69) and co-stimulation (CD86) across species using whole blood or isolated cells (Table 2). In mouse, anti-IgM-induced B cell proliferation is also potently blocked. These results confirm and extend published findings with PI3Kδ deficient mice and PI3Kδ selective tool compounds.^{33,34} The effects of CDZ173 on T cell responses are shown in Table 2. The mixed lymphocyte reaction (MLR) is a model for allogeneic T cell activation *in vitro*. The MLR with both human peripheral blood mononuclear cells (PBMCs) and mouse splenocytes is potently inhibited by CDZ173. The aCD3-stimulated proliferation of T cells from human PBMC is also inhibited, and the reduced dependency on PI3Kδ in the presence of aCD28 co-stimulation could be confirmed.³³ The differentiation of murine and human aCD3/aCD28 mAb-stimulated T cells into Th2 or Th17 cells is significantly blocked. In summary, CDZ173 potently blocks PI3Kδ dependent signaling in B and T cells across species and matrices.

CDZ173 shows a 30-fold cellular selectivity over PI3Kα (Table 1, cellular assay section in Supporting Information) which translates to a preservation of insulin homeostasis in mice up to a dose as high as 100 mg/kg bid (Supplementary Figure 9). While the cellular isoform selectivity against PI3Kα and β was determined in Rat-1 cells as already described, PI3Kγ activity has to be tested

1 differently due to its distinct signaling downstream of GPCR. We
2 measured the PI3K γ -dependent activation of U937 monocytes by
3 the GPCR-ligand MIP-1 α , and CDZ173 showed no activity up to
4 the highest test concentration ($IC_{50} > 7.4 \mu M$). In addition, the
5 cellular activity on PI3K γ was assessed via the activation of
6 mouse bone marrow-derived mast cells (BMMCs) stimulated with
7 adenosine where CDZ173 was a very weak inhibitor ($IC_{50} = 7.8$
8 μM). When tested in biochemical assays against the Class III
9 PI3K Vps34, and enzymes of the wider PI3K family (mTOR and
10 PI4K), CDZ173 was inactive up to the highest test concentration
11 ($IC_{50} > 9.1 \mu M$). Whilst DNA-PK was moderately inhibited by
12 CDZ173 (biochemical $IC_{50} = 0.88 \mu M$), this activity did not trans-
13 late to an inhibition of p53 in a stressed p53RE-bla HCT116 re-
14 porter cell line further down in the pathway of DNA-repair ($IC_{50} >$
15 $3 \mu M$).

16 CDZ173 showed no activity up to the highest test concentration
17 when tested against CYP isoform assays (3A3, 2D9, 2D6, 2C9),³⁵
18 a panel of ion channels (including hERG)³⁶ and a protease panel.
19 In a panel of 50 safety related targets (GPCRs, ion channels,
20 transporters), CDZ173 only showed measurable activity for
21 hPDE4D ($IC_{50}=4.7 \mu M$) and 5HT2B ($IC_{50}=7.7 \mu M$). Furthermore,
22 CDZ173 was tested against a panel of 442 diverse ser-
23 ine/threonine, tyrosine- and lipid kinases utilizing DiscoverX'
24 KINOMEScan® technology at $10 \mu M$. The only kinase that was
25 inhibited by CDZ173 (in addition to the expected Class I PI3Ks)
26 was RPS6KA5 (76% inhibition, no cellular follow-up as no nega-
27 tive impact on safety/tolerability was anticipated).

28 The pharmacokinetic profile of CDZ173 is shown in Table 3. In
29 general, the compound is absorbed very quickly across species as
30 can be seen by an early T_{max} of the oral profiles. Whereas clear-
31 ance is low to moderate in rats and monkeys, it was found that
32 clearance in dogs is very low resulting in a very high exposure in
33 blood. As dog plasma protein binding is very high ($>99\%$) and
34 restricting distribution of the compound into tissue ($V_{ss} = 0.3$
35 $L \cdot kg^{-1}$), dogs were excluded as a potential species for toxicologi-
36 cal studies. In contrast to compound **1a**,³⁰ CDZ173 did not show
37 underproportional exposure increase comparing 3 and 30 mg/kg
38 doses in rats.

39 Because of its favourable pharmacokinetic profile in rodents and
40 monkeys, we tested CDZ173 in various *in vivo* settings, starting
41 with PK/PD experiments. In rats, CDZ173 inhibits *ex vivo* anti-
42 IgM/IL-4 -induced proximal pAKT formation in rats in a concen-
43 tration- and time-dependent manner (see Supplementary Figure
44 1). Plotting total blood exposure against the PD effect, an $EC_{50} =$
45 83 nM ($EC_{50} \text{ free} = 5 \text{ nM}$, rat PPB = 94%) was calculated which
46 is in agreement with the *in vitro* rat whole blood B cell activation
47 assay result ($IC_{50} = 99 \text{ nM}$; Table 1). In cynomolgus monkeys, the
48 *ex vivo* activation of CD20+ B cells (anti-IgM/IL-4 stimulated
49 pAKT) was inhibited with an EC_{50} of ca. 140 nM (see Supple-
50 mentary Figure 2). As for rat, the exposure/concentration-
51 response profiles are in agreement with the *in vitro* whole blood
52 assay result ($IC_{50} = 84 \text{ nM}$, Table 2). The concentration-dependent
53 PD effect of CDZ173 translated into a dose dependent pharmaco-
54 logical inhibition of PI3K δ as demonstrated by inhibition of the
55 generation of antigen-specific antibody responses to sheep red
56 blood cells (SRBC) in rat (Figure 2). Encouraged by these results,
57 CDZ173 was tested in a rat model of collagen-induced arthritis
58 (rCIA) to assess the correlation of autoantibody levels with reduc-
59 tion of clinical symptoms and histological parameters. CDZ173
60 significantly inhibited pathogenic anti-rat collagen antibodies,
paw swelling, inflammatory cell infiltration, proteoglycan loss
and joint erosion when dosing started before disease onset. Full
efficacy was seen with doses as low as 3 mg/kg b.i.d (Supplemen-
tary Figures 3-6). In a therapeutic setting, where CDZ173 was
administered when significant paw swelling was already evident,

a dose of 10 mg/kg b.i.d. significantly ameliorated disease param-
eters and strongly reduced the degree of established autoantibody
responses (Figure 3 and Supplementary Figure 7). The PK profile
and the dose normalized AUC observed in the multiple dose ex-
periments was comparable to data obtained from single dose PK
studies in naive animals. In an ozone-induced lung inflammation
model in mice, CDZ173 dose-dependently inhibited the increase
in bronchoalveolar lavage (BAL) neutrophil and macrophage
numbers with ED_{50} values of 16 mg/kg and 40 mg/kg , respective-
ly (Supplementary Figure 8). There was no effect on the ozone-
induced plasma leakage, as measured by the increased BAL se-
rum albumin levels (data not shown). In all presented preclinical
multi-dose pharmacology studies, CDZ173 was well tolerated and
there were no apparent signs of toxicity.

Taken together, the *in vitro* properties and the results in prelini-
cal models of autoimmune and inflammatory diseases demon-
strate the potential of CDZ173 to act as a therapeutic for immune-
mediated diseases. Because of the big structural differences to the
first-generation of clinical PI3K δ and/or PI3K $\gamma\delta$ -selective inhibi-
tors, CDZ173 could favourably differentiate in terms of its safety
profile. After supportive preclinical toxicology studies and a suc-
cessful phase I clinical campaign, CDZ173 (leniolisib) is currently
being explored in clinical trials for APDS (ClinicalTrials.gov
identifier: NCT02435173) and primary Sjögren's Syndrome
(NCT02775916).

ASSOCIATED CONTENT

Supporting Information

Full descriptions of all biological assays and *in vivo* studies. Char-
acterization of all compounds. Full experimental procedures for
the sequence leading to CDZ173. Crystallographic data collection
and refinement statistics for crystal structures. This material is
available free of charge via the Internet at <http://pubs.acs.org>.

Accession Codes

PDB code for the X-ray crystal structure described in this study
has been deposited in the Protein Data Bank under the accession
code 5O83.

AUTHOR INFORMATION

Corresponding Authors

*(K.H.) Tel: +41 79 6181814. E-mail: klemens.hoegenauer@novartis.com.

*(N.S.) Tel: +41 79 8451506. E-mail: nico-las.soldermann@novartis.com.

Notes

The authors declare no competing financial interests.

ACKNOWLEDGMENTS

We thank C. Hebach, I. Lewis, A. von Matt for their synthetic and
medicinal chemistry contributions, I. Adam, I. Jeulin, D. Rageot,
B. Thai and V. Tuccini for their contributions in compound syn-
thesis, J. Trappe, D. d'Orazio, D. Kempf, C. Guntermann, F.
Ecoeur, D. Fabbro, D. Haasen, A. Hinz and P. Schmutz for their
efforts towards developing and performing biochemical and cellu-
lar assays, A. Trifilieff, R. Puljic, C. Schnell, C. Fritsch, U.
McKeever, C. Gfell, D. Buffet, S. Bolliger, R. Keller, S. Bay for
in vivo pharmacology, G. Wiecezorek, and N. Mamber for histolo-
gy, C. Beerli and B. Urban, P. Ramstein, W. Gertsch, S.
Desrayaud, J. Hengy, S. Widmer, I.R. Mueller, J. Kamholz, R.

Endres, A. Geisser, F.P. Cordoba, A. Kunkler, G. Laue, C. Textor, and A. Cattini for pharmacokinetic assay work, B. Shrestha for protein expression, R. Elling for crystallography support, K. Beltz and P. Santos for CDZ173 developability assessment as well as J. Wagner and G. Weckbecker for scientific guidance. We are grateful to the MX beamline team at the Swiss Light Source (PSI Villigen, Switzerland) for outstanding support at the beamline and Expose GmbH (Switzerland) for diffraction data collection.

ABBREVIATIONS

APDS, activated PI3K δ syndrome; BAL, bronchoalveolar lavage; BAV, absolute oral bioavailability; BMMC, bone marrow-derived mast cells; CIA, collagen-induced arthritis; CYP, cytochrome P450; GPCR, G protein-coupled receptor; hERG, human ether- α -go-go-related gene; MLR, mixed lymphocyte reaction; THPP, 5,6,7,8-tetrahydropyrido[4,3-d]pyrimidine; mTOR, mechanistic Target Of Rapamycin; PAMPA, parallel artificial membrane permeability assay; PASLI, p110 delta activating mutation causing senescent T cells, lymphadenopathy, and immunodeficiency; PBMC, peripheral blood mononuclear cells; PI3K, Phosphoinositide-3-kinase; SAR, structure-activity relationship; SRBC, sheep red blood cell(s); tPSA, topological polar surface area.

REFERENCES

- (1) Cantley, L. C. The Phosphoinositide 3-Kinase Pathway. *Science* **2002**, *296* (5573), 1655–1657.
- (2) Vanhaesebroeck, B.; Guillermet-Guibert, J.; Graupera, M.; Bilanges, B. The Emerging Mechanisms of Isoform-Specific PI3K Signaling. *Nat. Rev. Mol. Cell Biol.* **2010**, *11* (5), 329–341.
- (3) Reif, K.; Okkenhaug, K.; Sasaki, T.; Penninger, J. M.; Vanhaesebroeck, B.; Cyster, J. G. Cutting Edge: Differential Roles for Phosphoinositide 3-Kinases, p110 γ and p110 δ , in Lymphocyte Chemotaxis and Homing. *J. Immunol.* **2004**, *173* (4), 2236–2240.
- (4) Martini, M.; Santis, M. C. D.; Braccini, L.; Gulluni, F.; Hirsch, E. PI3K/AKT Signaling Pathway and Cancer: An Updated Review. *Ann. Med.* **2014**, *46* (6), 372–383.
- (5) Brown, J. R. The PI3K Pathway: Clinical Inhibition in Chronic Lymphocytic Leukemia. *Semin. Oncol.* **2016**, *43* (2), 260–264.
- (6) Park, S. J.; Lee, K. S.; Kim, S. R.; Min, K. H.; Moon, H.; Lee, M. H.; Chung, C. R.; Han, H. J.; Puri, K. D.; Lee, Y. C. Phosphoinositide 3-Kinase δ Inhibitor Suppresses Interleukin-17 Expression in a Murine Asthma Model. *Eur. Respir. J.* **2010**, *36* (6), 1448–1459.
- (7) Sadhu, C.; Dick, K.; Tino, W. T.; Staunton, D. E. Selective Role of PI3K δ in Neutrophil Inflammatory Responses. *Biochem. Biophys. Res. Commun.* **2003**, *308* (4), 764–769.
- (8) Brown, J. M.; Wilson, T. M.; Metcalfe, D. D. The Mast Cell and Allergic Diseases: Role in Pathogenesis and Implications for Therapy. *Clin. Exp. Allergy* **2008**, *38* (1), 4–18.
- (9) Sriskantharajah, S.; Hamblin, N.; Worsley, S.; Calver, A. R.; Hessel, E. M.; Amour, A. Targeting Phosphoinositide 3-Kinase δ for the Treatment of Respiratory Diseases. *Ann. N. Y. Acad. Sci.* **2013**, *1280* (1), 35–39.
- (10) Amour, A.; Barton, N.; Cooper, A. W. J.; Inglis, G.; Jamieson, C.; Luscombe, C. N.; Morrell, J.; Peace, S.; Perez, D.; Rowland, P.; Tame, C.; Uddin, S.; Vitulli, G.; Wellaway, N. Evolution of a Novel, Orally Bioavailable Series of PI3K δ Inhibitors from an Inhaled Lead for the Treatment of Respiratory Disease. *J. Med. Chem.* **2016**, *59* (15), 7239–7251.
- (11) Erra, M.; Taltavull, J.; Gréco, A.; Bernal, F. J.; Caturla, J. F.; Gràcia, J.; Domínguez, M.; Sabaté, M.; Paris, S.; Soria, S.; Hernández, B.; Armengol, C.; Cabedo, J.; Bravo, M.; Calama, E.; Miralpeix, M.; Lehner, M. D. Discovery of a Potent, Selective, and Orally Available PI3K δ Inhibitor for the Treatment of Inflammatory Diseases. *ACS Med. Chem. Lett.* **2017**, *8* (1), 118–123.
- (12) Bartok, B.; Boyle, D. L.; Liu, Y.; Ren, P.; Ball, S. T.; Bugbee, W. D.; Rommel, C.; Firestein, G. S. PI3 Kinase δ Is a Key Regulator of Synovocyte Function in Rheumatoid Arthritis. *Am. J. Pathol.* **2012**, *180* (5), 1906–1916.
- (13) Taher, T. E.; Parikh, K.; Flores-Borja, F.; Mletzko, S.; Isenberg, D. A.; Peppelenbosch, M. P.; Mageed, R. A. Protein Phosphoryla-

tion and Kinome Profiling Reveal Altered Regulation of Multiple Signaling Pathways in B Lymphocytes from Patients with Systemic Lupus Erythematosus. *Arthritis Rheum.* **2010**, *62* (8), 2412–2423.

(14) Suárez-Fueyo, A.; Barber, D. F.; Martínez-Ara, J.; Zea-Mendoza, A. C.; Carrera, A. C. Enhanced Phosphoinositide 3-Kinase δ Activity Is a Frequent Event in Systemic Lupus Erythematosus That Confers Resistance to Activation-Induced T Cell Death. *J. Immunol.* **2011**, *187* (5), 2376–2385.

(15) Randis, T. M.; Puri, K. D.; Zhou, H.; Diacovo, T. G. Role of PI3K δ and PI3K γ in Inflammatory Arthritis and Tissue Localization of Neutrophils. *Eur. J. Immunol.* **2008**, *38* (5), 1215–1224.

(16) Suárez-Fueyo, A.; Rojas, J. M.; Cariaga, A. E.; García, E.; Steiner, B. H.; Barber, D. F.; Puri, K. D.; Carrera, A. C. Inhibition of PI3K δ Reduces Kidney Infiltration by Macrophages and Ameliorates Systemic Lupus in the Mouse. *J. Immunol.* **2014**, *193* (2), 544–554.

(17) Angulo, I.; Vadas, O.; Garçon, F.; Banham-Hall, E.; Plagnol, V.; Leahy, T. R.; Baxendale, H.; Coulter, T.; Curtis, J.; Wu, C.; Blake-Palmer, K.; Perisic, O.; Smyth, D.; Maes, M.; Fiddler, C.; Juss, J.; Cilliers, D.; Markelj, G.; Chandra, A.; Farmer, G.; Kielkowska, A.; Clark, J.; Kracker, S.; Debré, M.; Picard, C.; Pellier, I.; Jabado, N.; Morris, J. A.; Barcenas-Morales, G.; Fischer, A.; Stephens, L.; Hawkins, P.; Barrett, J. C.; Abinun, M.; Clatworthy, M.; Durandy, A.; Doffinger, R.; Chilvers, E. R.; Cant, A. J.; Kumararatne, D.; Okkenhaug, K.; Williams, R. L.; Condliffe, A.; Nejentsev, S. Phosphoinositide 3-Kinase δ Gene Mutation Pre-disposes to Respiratory Infection and Airway Damage. *Science* **2013**, *342* (6160), 866–871.

(18) Lucas, C. L.; Kuehn, H. S.; Zhao, F.; Niemela, J. E.; Deenick, E. K.; Palendira, U.; Avery, D. T.; Moens, L.; Cannons, J. L.; Biancalana, M.; Stoddard, J.; Ouyang, W.; Frucht, D. M.; Rao, V. K.; Atkinson, T. P.; Agharabimi, A.; Hussey, A. A.; Folio, L. R.; Olivier, K. N.; Fleisher, T. A.; Pittaluga, S.; Holland, S. M.; Cohen, J. I.; Oliveira, J. B.; Tangye, S. G.; Schwartzberg, P. L.; Lenardo, M. J.; Uzel, G. Dominant-Activating Germline Mutations in the Gene Encoding the PI(3)K Catalytic Subunit p110 δ Result in T Cell Senescence and Human Immunodeficiency. *Nat. Immunol.* **2014**, *15* (1), 88–97.

(19) Marone, R.; Cmiljanovic, V.; Giese, B.; Wymann, M. P. Targeting Phosphoinositide 3-kinase—Moving towards Therapy. *Biochim. Biophys. Acta BBA - Proteins Proteomics* **2008**, *1784* (1), 159–185.

(20) Gold, M. R.; Puri, K. D. Selective Inhibitors of Phosphoinositide 3-Kinase Delta: Modulators of B-Cell Function with Potential for Treating Autoimmune Inflammatory Diseases and B-Cell Malignancies. *Front. Immunol.* **2012**, *3*.

(21) Hawkins, P. T.; Stephens, L. R. PI3K Signalling in Inflammation. *Biochim. Biophys. Acta BBA - Mol. Cell Biol. Lipids* **2015**, *1851* (6), 882–897.

(22) Studies published 2016 or earlier are cited in reference 31.

(23) Bhide, R. S.; Neels, J.; Qin, L.-Y.; Ruan, Z.; Stachura, S.; Weigelt, C.; Sack, J. S.; Stefanski, K.; Gu, X.; Xie, J. H.; Goldstine, C. B.; Skala, S.; Pedicord, D. L.; Ruepp, S.; Dhar, T. G. M.; Carter, P. H.; Salter-Cid, L. M.; Poss, M. A.; Davies, P. Discovery and SAR of pyrrolo[2,1-f][1,2,4]triazin-4-Amines as Potent and Selective PI3K δ Inhibitors. *Bioorg. Med. Chem. Lett.* **2016**, *26* (17), 4256–4260.

(24) Gonzalez-Lopez de Turiso, F.; Hao, X.; Shin, Y.; Bui, M.; Campuzano, I. D. G.; Cardozo, M.; Dunn, M. C.; Duquette, J.; Fisher, B.; Foti, R. S.; Henne, K.; He, X.; Hu, Y.-L.; Kelly, R. C.; Johnson, M. G.; Lucas, B. S.; McCarter, J.; McGee, L. R.; Medina, J. C.; Metz, D.; San Miguel, T.; Mohn, D.; Tran, T.; Vissinga, C.; Wannberg, S.; Whittington, D. A.; Whoriskey, J.; Yu, G.; Zalameda, L.; Zhang, X.; Cushing, T. D. Discovery and in Vivo Evaluation of the Potent and Selective PI3K δ Inhibitors AM-0687 and AM-1430. *J. Med. Chem.* **2016**, *59* (15), 7252–7267.

(25) Marcoux, D.; Qin, L.-Y.; Ruan, Z.; Shi, Q.; Ruan, Q.; Weigelt, C.; Qiu, H.; Schieven, G.; Hynes, J.; Bhide, R.; Poss, M.; Tino, J. Identification of Highly Potent and Selective PI3K δ Inhibitors. *Bioorg. Med. Chem. Lett.* **2017**, *27* (13), 2849–2853.

(26) Patel, L.; Chandrasekhar, J.; Evarts, J.; Forseth, K.; Haran, A. C.; Ip, C.; Kashishian, A.; Kim, M.; Koditek, D.; Koppenol, S.; Lad, L.; Lepist, E.-I.; McGrath, M. E.; Perreault, S.; Puri, K. D.; Villaseñor, A. G.; Somoza, J. R.; Steiner, B. H.; Therrien, J.; Treiberg, J.; Phillips, G. Discovery of Orally Efficacious Phosphoinositide 3-Kinase δ Inhibitors with Improved Metabolic Stability. *J. Med. Chem.* **2016**, *59* (19), 9228–9242.

(27) Patel, L.; Chandrasekhar, J.; Evarts, J.; Haran, A. C.; Ip, C.; Kaplan, J. A.; Kim, M.; Koditek, D.; Lad, L.; Lepist, E.-I.; McGrath, M. E.; Novikov, N.; Perreault, S.; Puri, K. D.; Somoza, J. R.; Steiner, B. H.; Stevens, K. L.; Therrien, J.; Treiberg, J.; Villaseñor, A. G.; Yeung, A.; Phillips, G. 2,4,6-Triaminopyrimidine as a Novel Hinge Binder in a Series of PI3K δ Selective Inhibitors. *J. Med. Chem.* **2016**, *59* (7), 3532–3548.

(28) Qin, L.-Y.; Ruan, Z.; Cherney, R. J.; Dhar, T. G. M.; Neels, J.; Weigelt, C. A.; Sack, J. S.; Srivastava, A. S.; Cornelius, L. A. M.; Tino, J. A.; Stefanski, K.; Gu, X.; Xie, J.; Susulic, V.; Yang, X.; Yarde-Chinn, M.; Skala, S.; Bosnius, R.; Goldstein, C.; Davies, P.; Ruepp, S.; Salter-Cid, L.; Bhide, R. S.; Poss, M. A. Discovery of 7-(3-(Piperazin-1-yl)phenyl)pyrrolo[2,1-f][1,2,4]triazin-4-Amine Derivatives as Highly Potent and Selective PI3K δ Inhibitors. *Bioorg. Med. Chem. Lett.* **2017**, *27* (4), 855–861.

(29) Terstiege, I.; Perry, M.; Petersen, J.; Tyrchan, C.; Svensson, T.; Lindmark, H.; Öster, L. Discovery of Triazole Aminopyrazines as a Highly Potent and Selective Series of PI3K δ Inhibitors. *Bioorg. Med. Chem. Lett.* **2017**, *27* (3), 679–687.

(30) Hoegenauer, K.; Soldermann, N.; Stauffer, F.; Furet, P.; Gravelleau, N.; Smith, A. B.; Hebach, C.; Hollingworth, G. J.; Lewis, I.; Gutmann, S.; Rummel, G.; Knapp, M.; Wolf, R. M.; Blanz, J.; Feifel, R.; Burkhardt, C.; Zécéri, F. Discovery and Pharmacological Characterization of Novel Quinazoline-Based PI3K Delta-Selective Inhibitors. *ACS Med. Chem. Lett.* **2016**, *7* (8), 762–767.

(31) Hoegenauer, K.; Soldermann, N.; Hebach, C.; Hollingworth, G. J.; Lewis, I.; von Matt, A.; Smith, A. B.; Wolf, R. M.; Wilcken, R.; Haasen, D.; Burkhardt, C.; Zécéri, F. Discovery of Novel Pyrrolidineoxy-Substituted Heteroaromatics as Potent and Selective PI3K Delta Inhibitors with Improved Physicochemical Properties. *Bioorg. Med. Chem. Lett.* **2016**, *26* (23), 5657–5662.

(32) <http://www.rcsb.org>, PDB ID=5T7F.

(33) Okkenhaug, K.; Bilancio, A.; Farjot, G.; Priddle, H.; Sancho, S.; Peskett, E.; Pearce, W.; Meek, S. E.; Salpekar, A.; Waterfield, M. D.; Smith, A. J. H.; Vanhaesebroeck, B. Impaired B and T Cell Antigen Receptor Signaling in p110 δ PI 3-Kinase Mutant Mice. *Science* **2002**, *297* (5583), 1031–1034.

(34) Clayton, E.; Bardi, G.; Bell, S. E.; Chantry, D.; Downes, C. P.; Gray, A.; Humphries, L. A.; Rawlings, D.; Reynolds, H.; Vigorito, E.; Turner, M. A Crucial Role for the p110 δ Subunit of Phosphatidylinositol 3-Kinase in B Cell Development and Activation. *J. Exp. Med.* **2002**, *196* (6), 753–763.

(35) Bell, L.; Bickford, S.; Nguyen, P. H.; Wang, J.; He, T.; Zhang, B.; Friche, Y.; Zimmerlin, A.; Urban, L.; Bojanic, D. Evaluation of Fluorescence- and Mass Spectrometry-Based CYP Inhibition Assays for Use in Drug Discovery. *J. Biomol. Screen.* **2008**, *13* (5), 343–353.

(36) Finlayson, K.; Turnbull, L.; January, C. T.; Sharkey, J.; Kelly, J. S. [3H]Dofetilide Binding to HERG Transfected Membranes: A Potential High Throughput Preclinical Screen. *Eur. J. Pharmacol.* **2001**, *430* (1), 147–148.

FIGURES AND TABLES

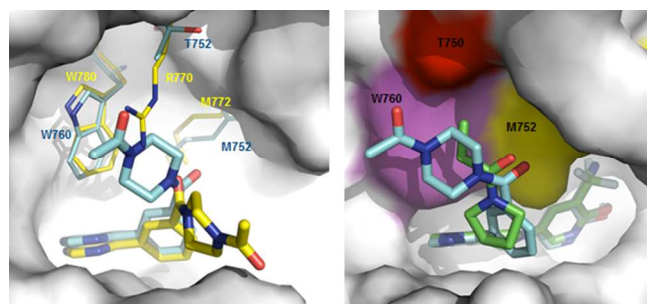


Figure 1. Left panel, Structural alignment of PI3K α and PI3K δ with compound **1a** bound to the ATP sites. The protein part of PI3K δ /compound **1a** (PDB 5IS5)³⁰ is depicted as grey surface. Amino acid side chains T750, M752, W760 and the inhibitor are represented as blue sticks for PI3K δ . The corresponding amino acid and inhibitor structures in PI3K α (PDB 5ITD)³⁰ are shown in yellow. Right panel, Comparison of the binding modes of CDZ173 (green sticks) and compound **1a** (blue sticks) to the active site of PI3K δ (grey surface with amino acids T750, M752 and W760 coloured in red, yellow and magenta, respectively).

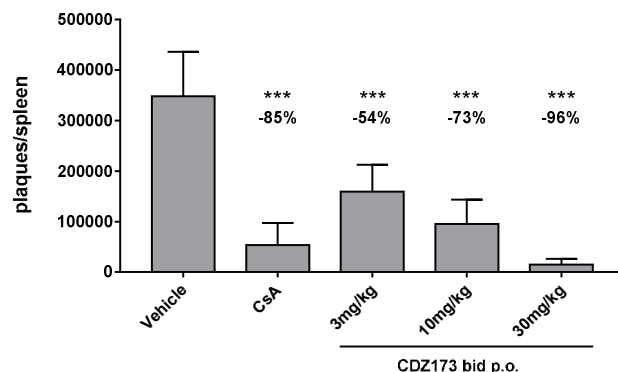


Figure 2. Dose-dependent inhibition of SRBC-specific IgM response by CDZ173 (error bars indicate SD); ***: $p < 0.001$ compared to vehicle (student's t-test, two-tailed distribution).

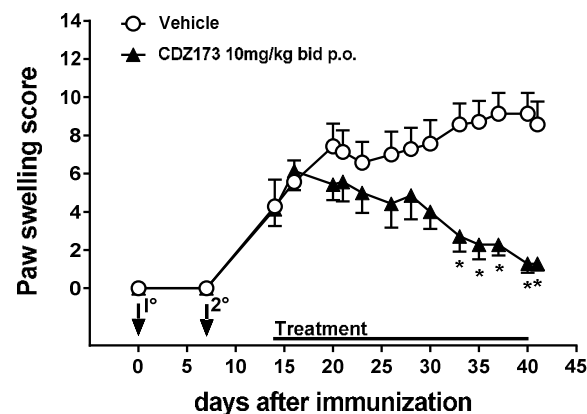
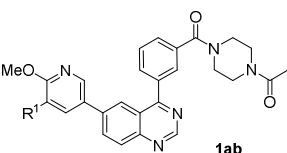
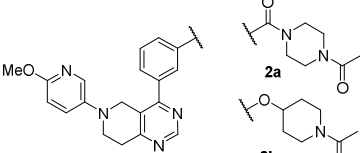
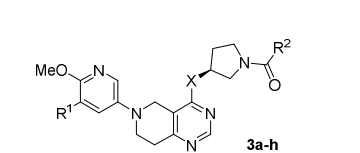

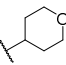
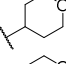
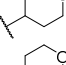
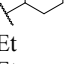


Figure 3. Inhibition of paw swelling in a therapeutic rat CIA experiment (dosing after disease onset, error bars indicate SEM). Antigen priming (1°) and boost (2°) indicated with arrows. Treatment period indicated with horizontal line at bottom of graph. * $p < 0.01$.

Table 1. Influence of 5,6,7,8-tetrahydropyrido[4,3-d]pyrimidine core introduction on biochemical/cellular potency, PI3K isoform selectivity and *in vitro* ADME parameters

																
	X	R ¹	R ²	biochemical IC ₅₀ [μM] ^a				cellular IC ₅₀ [μM] ^{a, d}			mCD86	rCD86	PAMP	HT-	RLM	HT-
				PI3Kα ^b	PI3Kβ ^b	PI3Kγ ^b	PI3Kδ ^c	PI3Kα	PI3Kβ	PI3Kδ	IC ₅₀ ^{a, e}	IC ₅₀ ^{a, f}	A	logP ^g	logP ^h	CL _{int} ^j
1a		CN		0.262	1.65	4.63	0.009	3.44	6.53	0.049	0.074	0.072	-5.5	2.8	63	0.21
1b		H		0.418	4.84	2.70	0.029	2.12	3.57	0.028	0.070	0.066	-4.9	2.7	115	>1.0
2a				6.94	>9.1	>9.1	0.065	>10	>10	2.63	nd	nd	-6.7	0.7	91	>1.0
2b				2.02	>9.1	>9.1	0.083	9.03	>10	0.374	nd	nd	-4.1	2.2	197	>1.0
3a	O	H	Et	6.66	8.94	>9.1	0.132	>10	>10	5.39	nd	nd	-3.7	2.2	35	>1.0
3b	O	CF ₃	Et	0.792	1.71	>9.1	0.027	2.60	3.11	0.131	nd	nd	-3.6	3.1	160	0.080
3c	O	Me		1.94	4.15	6.60	0.076	6.49	6.79	0.143	0.098	0.092	-4.2	1.7	60	>1.0
3d	O	CF ₃		0.590	1.33	>9.1	0.028	3.55	3.58	0.037	0.084	0.058	-3.7	2.2	149	0.27
3e	NH	Me		0.373	2.02	3.29	0.030	6.19	9.87	0.358	0.091	0.074	-5.9	2.6	22	>1.0
3f	NH	CF ₃		0.044	0.300	1.06	0.004	2.15	3.99	0.053	0.015	0.016	-5.5	2.9	41	0.24
3g	NH	Me	Et	0.651	0.951	nd	0.020 ^b	7.41	7.91	0.246	0.087	0.073	-5.7	2.8	nd	>1.0
3h*	NH	CF ₃	Et	0.244	0.424	2.23	0.011	1.67	2.25	0.056	0.048	0.099	-4.5	3.2	55	0.32

^aMean of a minimum of two independent experiments; standard deviation for pIC₅₀ values <0.3; ^bKGlo format; ^cADAPTA format (values comparable to KGlo); ^dinhibition of pAkt formation in Rat-1 cells; ^einhibition of anti-IgM induced mCD86 expression on mouse splenocytes; ^finhibition of anti-IgM/IL-4 induced rCD86 expression in 50% rat blood; ^geffective permeability [10⁻⁶ cm·sec⁻¹] (pH = 6.8), n=1; ^hHigh-throughput logP measurement with immobilized artificial membranes, n=1; ⁱintrinsic clearance in incubations of rat liver microsomes [μL·min⁻¹·mg⁻¹ protein], n=1; ^jHigh-throughput equilibrium solubility determination [mM] (pH = 6.8); nd = not determined; *CDZ173 (leniolisib)

Table 2. Cellular inhibition of PI3Kδ -dependent B and T cell functions in different species by CDZ173.

Species	B cells ^a								T cells							
	human ^b				cyno ^b				mouse ^d				human ^e			
Stimulus	aIgM	aIgM/IL-4	aIgM	aIgM/IL-4	aIgM	aIgM/IL-4	aIgM	aIgM/IL-4	aIgM	Allo MLR ^f	aCD3 ^g	aCD3/aCD28 ^f	aIgM	Allo MLR ^f	aCD3/aCD28 ^f	aIgM
Readout	pAKT	CD86	CD69	pAKT	pAKT	CD86	Prol. ^g	CD86	Prol. ^g	Prol. ^g	Th2	Th17	Prol. ^g	Prol. ^g	Th2	Th17
IC ₅₀ [μM]	0.144	0.202	0.193	0.084	0.150	0.099	0.007	0.048	0.079	0.159	0.095	0.073	1.15	0.033	0.010	0.101

^aData from at least two independent experiments are shown; standard deviation for pIC₅₀ values <0.3; ^bmeasured in 90% whole blood; ^cmeasured in 50% whole blood; ^dmeasured in splenocytes; ^emeasured in PBMCs; ^fmean of at least four independent experiments; ^gproliferation (Prol.) measured as ³H-Thymidine uptake

Table 3. PK parameters^a for CDZ173 (crystalline free base).

Species	Rat ^b	Rat ^b	Rat ^b	Dog ^c	Dog ^c	Monkey ^d	Monkey ^d
Dose [mg·kg ⁻¹]	1 (iv)	3 (po)	30 (po)	0.1 (iv)	0.3 (po)	0.1 (iv)	0.3 (po)
CL [mL·min ⁻¹ ·kg ⁻¹]	28 (3)			2 (1)		17 (2)	
V _{ss} [L·kg ⁻¹]	3.1 (0.8)			0.3 (0.1)		0.6 (0.1)	
t _{1/2} term. [h]	1.8 (0.3)			1.5 (0.4)		0.7 (0.4)	
AUC d.n. ^e [nM·h]	1355 (158)	1165 (27)	2107 (655)	20120 (7720)	11690 (6277)	2250 (290)	297 (107)
BAV [%]		86 (2)	>100		58 (31)		13 (5)
C _{max} d.n. ^e [nM]		391 (161)	334 (105)		3410 (1347)		213 (180)
T _{max} [h]		0.4 (0.1)	<0.25		0.7 (0.3)		<0.5

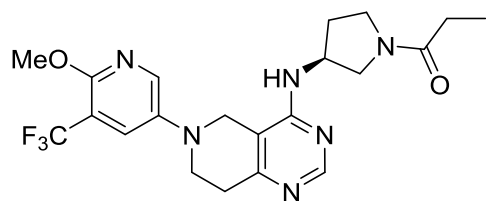
^aMean values with standard deviation in brackets; ^bfemale, n=4; ^cmale, n=3; ^done female, two male; ^ed.n. = dose normalized to 1 mg·kg⁻¹

==== For Table of Contents Use Only ====

Discovery of CDZ173 (leniolisib), Representing a Structurally Novel Class of PI3K Delta-Selective Inhibitors

Klemens Hoegenauer^{*a}, Nicolas Soldermann^{*a}, Frédéric Zécari^a, Ross S. Strang^a, Nadege Graveleau^a, Romain M. Wolf^a, Nigel G. Cooke^a, Alexander B. Smith^a, Gregory J. Hollingworth^a, Joachim Blanz^b, Sascha Gutmann^c, Gabriele Rummel^c, Amanda Littlewood-Evans^d, Christoph Burkhardt^d

^aGlobal Discovery Chemistry, ^bPK Sciences, ^cChemical Biology and Therapeutics, ^dAutoimmunity, Transplantation and Inflammation, Novartis Institutes for BioMedical Research, Novartis Campus, CH4002 Basel, Switzerland



CDZ173 (Leniolisib)

1
2
3
4
5
6
7
8
9
10
11
12
13
14
15
16
17
18
19
20
21
22
23
24
25
26
27
28
29
30
31
32
33
34
35
36
37
38
39
40
41
42
43
44
45
46
47
48
49
50
51
52
53
54
55
56
57
58
59
60